Sens. & Instrumen. Food Qual. (2007) 1:151–159
DOI 10.1007/s11694-007-9017-x

ORIGINAL PAPER

Hyperspectral reflectance and fluorescence line-scan imaging for online defect and fecal contamination inspection of apples

Moon Sung Kim · Yud-Ren Chen · Byoung-Kwan Cho · Kuanglin Chao · Chun-Chieh Yang · Alan M. Lefcourt · Diane Chan

Received: 31 December 2006 / Accepted: 14 June 2007 / Published online: 25 July 2007

Abstract We have recently developed a rapid online line-scan imaging system capable of both hyperspectral Vis/NIR reflectance and fluorescence in the Vis with UV-A excitation. The hyperspectral online line-scan system was integrated with a commercial apple-sorting machine and evaluated to inspect apples for fecal contamination and defects at a processing line speed of over three apples per second. Results showed that fluorescence imaging (using a two-band ratio) could achieve detection of fecal spots on artificially contaminated apples with a 100% detection rate and no false positives regardless of the presence of defects. A NIR two-band reflectance ratio coupled with a simple classification method based on the mean intensity and homogeneity of the ratio achieved a 99.5% apple defect classification accuracy with a false positive rate of only 2%. The presented NIR processing regime overcame the presence of stem/calyx on apples that typically has been a problematic source for false positives in the detection of defects. The most significant and important outcome of this investigation is a line-scan inspection system that can potentially provide the capability for current sorting mechanisms, such as by size and color, as well as additional sorting for quality and safety attributes of food products. This line-scan based online imaging system offers great potential as a value-added dynamic inspection system due to its capability for multi-tasking to meet a variety of inspection objectives. A multi-tasking inspection system that can meet current industry sorting needs with the added benefit of safety inspection without requiring significant modification of existing infrastructure or incurring significant costs may lead the apple industry to consider adopting voluntary measures to further enhance safe production and processing of fruits.

Keywords Hyperspectral imaging · Reflectance · Fluorescence · Online inspection · Fecal contamination · Defects · Apples

Company and product names are used for clarity and do not imply any endorsement by U.S. Department of Agriculture to the exclusion of other comparable products.

M. S. Kim (✉) · Y.-R. Chen · K. Chao · A. M. Lefcourt · D. Chan
Instrumentation and Sensing Laboratory, USDA, Agricultural Research Service, ANRI, Powder Mill Rd. Bldg 303, BARC-East, Beltsville, MD 20705, USA
e-mail: kimm@ba.ars.usda.gov

B.-K. Cho
Bioindustrial Machinery Engineering, Chungnam National University, Daejeon 305-764, Korea

C.-C. Yang
Biosystems and Agricultural Engineering, University of Kentucky, Lexington, KY 40546, USA

Introduction

The safe production of foods to minimize foodborne illness is a concern for both the general public and the entire food industry [1]. Contamination of food products by animal fecal matter is recognized as a major culprit for pathogenic *E. coli* O157:H7 [2, 3]. Fruits with defects, such as cuts, lesions, and rots that are known to provide favorable ecological niches for bacterial growth [4, 5], are also safety concerns.

Opto-electronic imaging techniques as rapid nondestructive sensing tools have been incorporated into agricultural production inspection. Various sensing techniques including the use of X-rays, RGB color, visible/near-infrared (Vis/NIR) reflectance, and fluorescence have been

investigated for potential use in online applications [6–14]. In particular, these optical imaging techniques hold great potential for rapid apple quality inspection. The most prevalent is reflectance in Vis/NIR portions of the spectrum, used in monochromatic, color (RGB), or multispectral regimes [15–17]. Furthermore, the efficacy of fluorescence imaging for postharvest food safety inspection for fecal contamination has been demonstrated using fruits artificially contaminated with a range of diluted animal feces [18–21].

In the apple processing industry, an online-based machine vision system is typically dedicated to performing a specific sorting task. Current commercial systems address sorting by size, shape, and color. The apple industry is in need of sorting methods for apples with defects such as fungal growth, cuts, lesions, bruises, rots, and insect damage. In order to achieve rapid sorting and meet inspection objectives for various quality and safety attributes, multiple machine vision systems may have been needed. For a single inspection system to meet a multiple inspection objectives, it needs to have the combination of (1) flexibility in employing sensing techniques, e.g., fluorescence and reflectance, (2) selectivity of multispectral bands, and (3) capabilities for simultaneous acquisition of multispectral bands. Researchers at the Instrumentation and Sensing Laboratory, USDA Agricultural Research Service, have recently designed and developed a rapid online line-scan imaging system capable of both hyperspectral Vis/NIR reflectance and fluorescence in the Vis with UV-A excitation. Recent advancements for sensitive low-light imaging devices and peripherals allow hyperspectral imaging of fast moving targets. Though redundant in spectral data, the online line-scan system provided a range of spectral data to evaluate apple inspection for a variety of quality and safety attributes. Thus, an experimental regime was designed to demonstrate the system as a potential means to address the inspection of apples for a variety of quality and safety concerns using a single imaging system.

In this paper, results obtained from the line-scan hyperspectral imaging system integrated with a commercial apple-sorting machine for detection of fecal contamination and defects on apples based on the fluorescence and reflectance imaging methods, respectively, are presented. To introduce the potential of the line-scan system as a multi-tasking machine vision platform for inspection of various safety and quality attributes, analyses were performed for detection of fecal contamination on apples regardless of the presence of defects, and detection of defects regardless of fecal contamination. No attempts were made to differentiate various defect types such as fungal growth, bruises, legions, and rots. For fecal contamination, apples were artificially contaminated with fresh cow feces.

Materials and methods

Hyperspectral line-scan imaging system

A hyperspectral line-scan imaging system that can capture both fluorescence and reflectance in the Vis/NIR regions of the spectrum was developed to inspect apples for quality and safety attributes. A schematic and a photo of the hyperspectral line-scan inspection system integrated with a commercial-grade apple-sorting machine (FMC Corp, Philadelphia, PA, USA) are shown in Fig. 1a and b, respectively. The line speed of the apple-sorting machine was adjusted to run at slightly over three apples per second. The sorting machine loads apples onto a conveyor/tray system to transport the apples. Each rectangular tray has a central circular depression to hold an apple while in transit and was painted with non-fluorescent, flat black paint to minimize background fluorescence emission and reflectance scattering.

The hyperspectral line-scan imaging system utilizes an electron-multiplying charge-coupled-device (EMCCD) imaging device (PhotonMAX, Roper Scientific, Inc., Trenton, NJ, USA). The EMCCD has 512 × 512 pixels and is thermoelectrically cooled down to –70 °C via a three-stage Peltier device. The imaging device is coupled with a 10 MHz (pixel-readout rate), 16-bit digitizer. An imaging spectrograph (ImSpector V10, Spectral Imaging Ltd., Oulu, Finland) and a C-mount lens (Rainbow CCTV S6X11, International Space Optics, S.A., Irvine, CA, USA) are attached to the EMCCD. The instantaneous field of view (IFOV) is limited to a thin line by the spectrograph aperture slit (50 μm). Through the slit, light from the scanned IFOV line is dispersed by a prism-grating-prism device and projected onto the EMCCD. Therefore, for each line-scan, a two-dimensional (spatial and spectral) image is created with the spatial dimension along the horizontal axis and the spectral dimension along the vertical axis of the EMCCD.

Interface software (WinView/32 version 2.5.19.0) provided by the EMCCD manufacturer was used for data acquisition. To increase imaging speed and to minimize the redundancy in the spectral imaging data, the original image size, 512 × 512 pixels, was reduced using 6 × 6 binning to produce an image size of 85 × 85 pixels. The 6 × 6 binning and the apple-sorting machine speed of 3 apples per second resulted in a spatial pixel resolution of approximately 2 mm^2. Furthermore, it should be noted that not all EMCCD pixels in the spectral (vertical) dimension were utilized; the light dispersed by the spectrograph did not span the full vertical width of the EMCCD. Thus, the effective spectral dimension was further reduced to 60 pixels (channels) spanning from approximately 400–1,000 nm with a channel interval of approximately 10 nm. A detailed description of spectral calibration is omitted for brevity (See [22]).

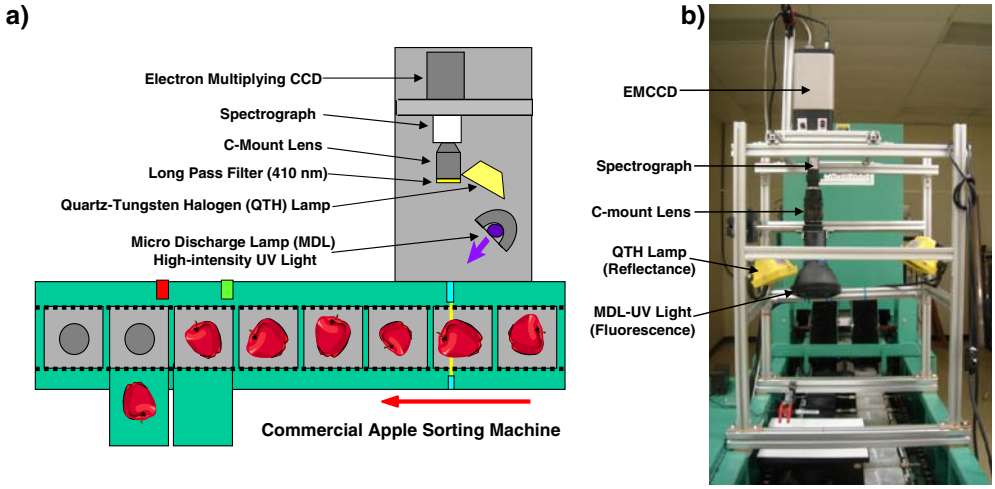

Fig. 1 (**a**) Schematic illustration, and (**b**) photo of online hyperspectral reflectance and fluorescence line-scan imaging system

The line-scan imaging system used two different independent continuous wave (CW) light sources: a pair of 150-w quartz-tungsten lamps were employed for reflectance imaging and a micro-discharge high intensity UV lamp with a diffuse filter (ML-3500, Spectronics Corp., Westbury, NY, USA) was employed for fluorescence imaging. Reflectance at wavelengths shorter than 450 nm was not used due to poor signal-to-noise ratio; the very low irradiance in that portion of the spectrum was an attribute of the quartz halogen light sources. With UV-A illumination, most biological materials exhibit fluorescence emissions between 400 and 700 nm. Thus, fluorescence spectra are presented only in that spectral range.

Image processing and analysis software was developed on a Microsoft (MS) Visual Basic (Version 6.0) platform in the MS Windows operating system. Using the downloaded hyperspectral image cube data, the software allows visualization of individual apple images and automated detection of feces-contaminated spots and defects as the stream of hyperspectral image cube data are accessed. Currently, the system data acquisition function is being incorporated into the software to achieve real-time visualization/detection.

A preliminary test suggested that over 50 apples per second could be processed using a computer with a 2 GHz processor. With the current imaging configuration, the data transfer rate (i.e., 10 MHz pixel readout rate) is one of the limiting factors that prevents the hyperspectral imaging system from processing more than three apples per second. The system can be configured to acquire only several spectral channels (multispectral/random track mode), which will markedly reduce the data volume per line-scan and result in higher spatial resolution. We are also in the process of updating the EMCCD to operate with a pixel readout rate of approximately 30 MHz.

Apples and animal feces

A batch of over 500 'Golden Delicious' apples originally intended for making unpasteurized apple cider and a second batch of over 500 Golden Delicious apples were obtained from a local orchard (O'Keefe's Orchard, Silver Spring, MD). The cider apples had been presorted by the orchard and included fruits with defects such as fungal infections (black pox and sooty blotch), bruises, cuts, lesions, and insect damage. The second batch contained normal apples exhibiting minimal blemishes, and had been destined for fresh consumption.

Fresh cow feces, of animals that had been fed feedstuffs containing green roughage, were collected from USDA farm facilities in Beltsville, MD. A thin cow feces spot (approximately 2 cm in diameter) was artificially created on each cider apple by smearing the cow feces on the apple using a spatula. Note that the smears of cow feces created transparent film-like coatings on the apples and, visually, were not easily discernable by human eye. A total of 60 cider apples were selected for treatment with cow feces but only 59 were actually treated, with 1 apple mistakenly left out.

Because the potential for contamination increases with the presence of defects such as cuts and lesions that present favorable ecological niches for bacterial growth [4, 5], the fecal contamination treatment was applied only to cider apples exhibiting defects. Online fluorescence images were acquired for 60 apples with defects prior to feces treatment, for the 59 feces-treated apples one day after the feces treatment, and again for these 59 apples after one month of cold storage. An additional 79 normal apples were also imaged as control samples, before and after one month of cold storage. For the fecal contamination inspection study, the total number of apple images used was 257, consisting of 118 fecal-contaminated apple images and 139 control apple images.

For investigation of defect detection, a total of 179 defect apples were imaged. The 59 cider apples that had been treated with fecal smears were included among the 179 images of apple defects used for this investigation. Previous investigation had shown that a thin transparent smear of cow feces could not be readily detected with reflectance imaging methods in the visible/NIR regions of the spectrum [8]. In addition, 196 normal apples with minimal blemishes were imaged as control samples.

Apples used in this investigation were selected randomly from their respective batches with no consideration for specific defect type. Based on visual observation, the defect samples appeared to encompass a variety of defect types and a range of degrees of defects. Individual feces-treated apples were purposely oriented on the sorting machine trays with the fecal smear spots facing the camera, while control apples were randomly positioned on the trays by the loading mechanism of the sorting machine.

Results and discussion

Fluorescence imaging for detection of fecal contamination

Representative fluorescence spectra from 400 to 700 nm were extracted from areas of hyperspectral images for two normal apple surfaces, a feces spot, a calyx region (shaded), and a rotted (defect) portion of an apple; these are shown in Fig. 2. Note that the individual spectra were obtained from individual regions of interest consisting of approximately 4–9 pixels each (averaged intensity per wavelength). With UV-A excitation, Golden Delicious apples typically exhibit a broad emission in the blue and green regions of the spectrum with maxima located approximately at 460 and 530 nm, respectively. Chlorophyll *a* fluorescence with emission maximum at near 680 nm is also observed from Golden Delicious apples. For the areas of apples coated with the transparent fecal smears, a blue shift in the chlorophyll *a* emission peak (e.g., 670 nm) is typically observed [23].

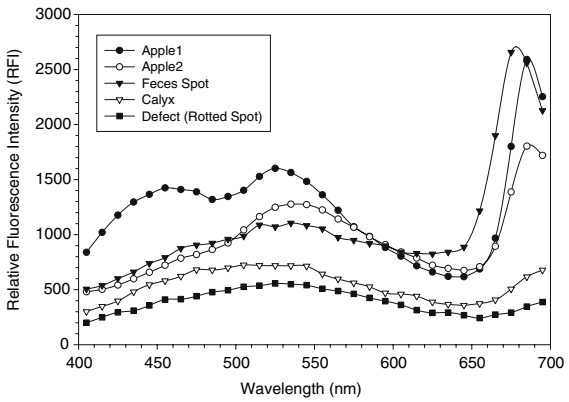

Fig. 2 Representative fluorescence spectra acquired using the online hyperspectral line-scan imaging system

Relative intensity variations dependent upon degree of fruit ripeness were observed. Furthermore, the relative intensity differences were wavelength dependent in that blue and red emissions compared to the green band for a well-ripened apple (Apple2) were lower than for a green apple (Apple1) in Fig. 2. The rotted spot and calyx region showed a broad and relatively low blue-green fluorescence and minimal chlorophyll *a* emission compared to the emissions of the greenish Golden Delicious apples. Responses of stem and adjacent shaded regions were also similar to those of calyx and rotted spots (Figure not shown).

Figure 3 shows fluorescence emission band images of representative samples at the 530 nm emission maximum in the green region (F530), at the 670 nm emission peak for bovine feces (F670), and at the 680 nm chlorophyll *a* emission peak (F680). In each of the three emission band images, normal apples (with minimal defects) are in the top row, while feces-treated defect apples (i.e., those exhibiting bruises and cuts, rotted areas, and fungal growths such as sooty blotch) are in the bottom row. The normal apples were imaged with apples randomly oriented by the sorting machine, while the feces-treated apples were positioned by hand to ensure that the fecal spots faced the camera. The imaging parameters used in this investigation, such as pixel readout rate and binning, and the sorting-line speed, resulted in approximately 900 pixels for a single apple image.

The fluorescence images show the defects and some stems as relatively dark spots compared to the surrounding normal apple surfaces. It is apparent that the concave features of the stem and calyx regions of the apples resulted in some shaded regions that were sometimes also observed as relatively darker spots, depending on the orientation of the apples. Apple-to-apple intensity variation was also observed for the emission regions under this investigation and was attributed to individual color and/or maturity differences.

We previously found a two-fluorescence band ratio to be an efficient multispectral image fusion method for detection of fecal contamination on apples [9, 19]. Compared to normal apple surfaces, feces spots have relatively lower and higher emission in the green and red (the blue-shift feces) wavelength regions, respectively, and thus a ratio of these two bands enhances the appearance of the fecal spots on apples. For calyx and rotted spots, green fluorescence responses compared to the fecal emission maximum in the red were relatively higher, and the ratio of the two bands yielded much smaller values than those for feces spots.

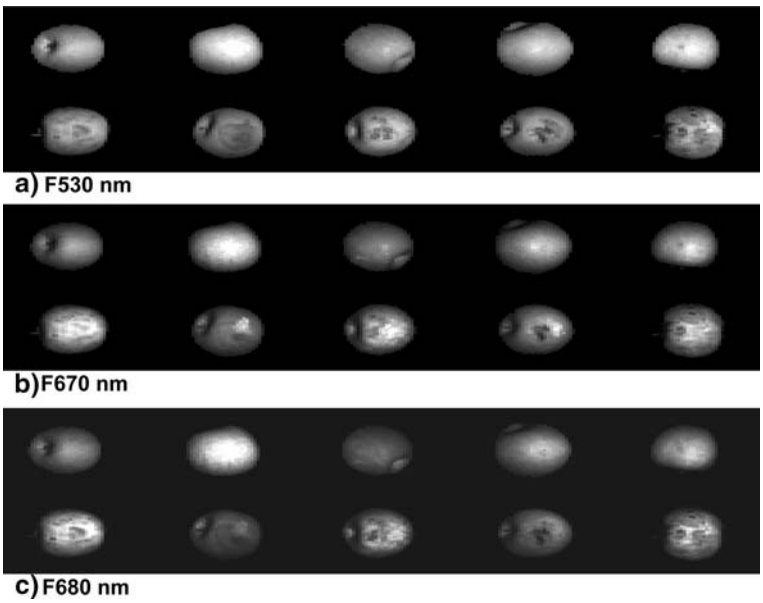

Fig. 3 Representative fluorescence images at (**a**) 530, (**b**) 670, and (**c**) 680 nm. Images were acquired with the apple-sorting machine line speed of three apples per second

A two-band ratio also reduced the spatial heterogeneity of normal apple surfaces, especially using a more blue-shifted red fluorescence band (e.g., 660 nm).

Prior to calculating the ratio values of the two-band images, a masking operation was performed to eliminate background portions of the images. Figure 4a shows a mask image for the apples shown in Fig. 3 that was created using the F660 band with a single threshold value (RFI of 330). Figure 4b shows the ratio image of 660 nm over 530 nm (F660/F530). Feces-treated spots that previously were not clearly visible in the individual emission images now appear as brighter, more distinct regions for the bottom row apples in the ratio image. In addition, the feces spots are brighter than the surrounding apple surfaces regardless of the presence of defects, fungal spots, and stem and calyx regions including the shaded regions. Figure 4c shows the binary image highlighting the regions of the feces contamination, obtained by subjecting the ratio image to a simple thresholding method using a global threshold value of 0.99. Based on the samples in this investigation, a 100% detection rate (118 feces-treated apples) was achieved, with no false positives (0 out of 139 normal apples). Fluorescence imaging techniques have consistently demonstrated very high detection rates for detecting animal fecal contamination on apples.

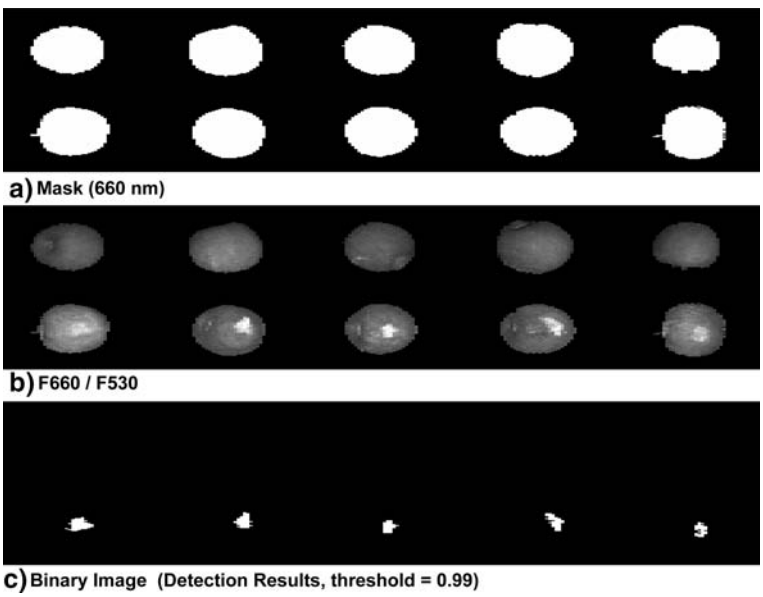

Fig. 4 (**a**) Binary mask image obtained using F660 nm image. (**b**) Representative fluorescence ratio image (660/530 nm) of samples. (**c**) Resultant binary image for feces-contaminated spots. Binary images for fecal contamination were obtained by the application of a simple thresholding method with a global threshold value of (0.99)

Reflectance imaging for detection of defects

Representative reflectance spectra from 450 to 1,000 nm extracted from areas of hyperspectral images for normal apple surfaces, stem and calyx regions, and from defect portions of Golden Delicious apples, are shown in Fig. 5. As for the fluorescence spectra shown in Fig. 2, each individual reflectance spectrum represents a region of interest consisting of approximately 4–9 pixels (averaged intensity per wavelength). Reflectance of Golden Delicious apples exhibited relatively high green reflectance at around 550 nm due to the green coloration, as well as a characteristic absorption of chlorophyll *a* in the red region of the spectrum with absorption maximum at around 670 nm.

Differences in the apples' natural green coloration affected reflectance responses in the green and red regions (e.g., Apple1 and Apple2 in Fig. 5). The reflectance spectra of some defects, rotted spots and fungal growth regions, although visually black in appearance, also exhibited varying degrees of the characteristic feature reminiscent of chlorophyll *a* absorption in the red region. The spectral reflectance responses were consistent in that the NIR slope between 750 and 800 nm was negative for the normal apples and positive for the defects. Stem and calyx areas exhibited reflectance responses similar to the defects.

The reflectance images at 600 nm (R600) and 800 nm (R800) in Fig. 6a and b, respectively, show representative normal apples in each top row and feces-treated defect apples in each bottom row. Note that these apples are different samples from those shown in the fluorescence images in Fig. 4. The defect portions (and the stem/calyx regions and shaded areas) of the samples exhibited relatively darker reflectance than the surrounding normal apple surfaces in the wavelength regions under investigation. Based on the spectral responses, a NIR two-band ratio using the 750 and 800 nm band pair may provide the greatest difference in ratio values between normal apple surfaces and defect portions (Fig. 6c). However, because of the spectral resemblance of apple stem and calyx regions to defects including rots, cuts, legions, and fungal growth, false positives are ever present, as evidenced in Fig. 6c.

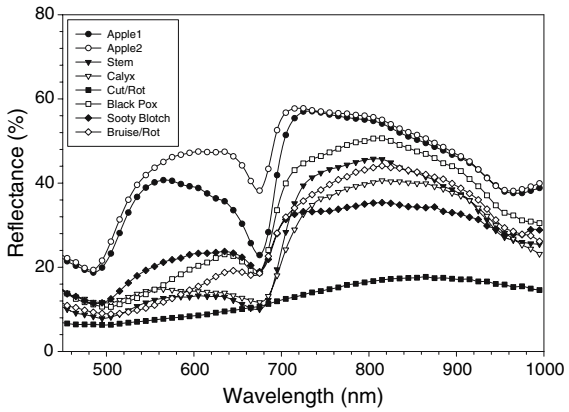

Fig. 5 Representative reflectance spectra acquired using the online hyperspectral line-scan imaging system

Briefly, because of the use of a grating in the spectrograph, a second-order effect is present in the longer wavelength region starting at approximately 800 nm. One of the considerations in selection of suitable bands in terms of multispectral band fusion is that the focal length (plane) of a camera lens is wavelength-dependent. To minimize artifacts, it is preferable to select two wavelengths in close proximity without overlapping spectral regions. In our case and based on the spectral characteristics of various apple surface conditions, two NIR bands at 750 and 800 nm, separated by only 50 nm, were chosen.

As suggested by Kim et al. [8], utilizing morphological image processing to eliminate false positives emanating from the stem/calyx regions would be computationally costly. Having knowledge of the location of calyx or stem in the image would be beneficial in morphologically based defect detection [24]. With the use of the NIR reflectance ratio image (Fig. 6c), we recognized that the ratio means and standard deviations for normal apples were significantly lower than for apples with defects, regardless of the presence of stem/calyx false positives (Fig. 7). In addition to the presence of the stem and/or calyx, the presence of defects obviously increased the mean ratio values and the spatial heterogeneity of the NIR ratio responses. Thus, the means and coefficients of variation of the ratio values, as a simple classification model input, were calculated for individual apples and subjected to SAS discriminant analysis (SAS version 8.0, Cary, NC; PROC DISCIM, linear model with one-cross out validation). This resulted in the correct classification of 98.0% of normal apples (4 out of 196 misclassified) and 99.4% of defects (1 out of 179 misclassified). The misclassification of some normal apples as defects might be attributed to those apples actually having some very minor defects/blemishes.

Utilizing a relatively fast data transfer board (i.e., pixel readout rate of 10 MHz), line-scan hyperspectral imaging of relatively fast moving targets was achieved. Both the spectral and spatial responses in fluorescence and reflectance and the results obtained in this investigation were analogous to data acquired in our previous laboratory studies using stationary or slower-moving samples.

Practical considerations

Technical potential

The most significant and important outcome of this investigation is the technical demonstration of a single

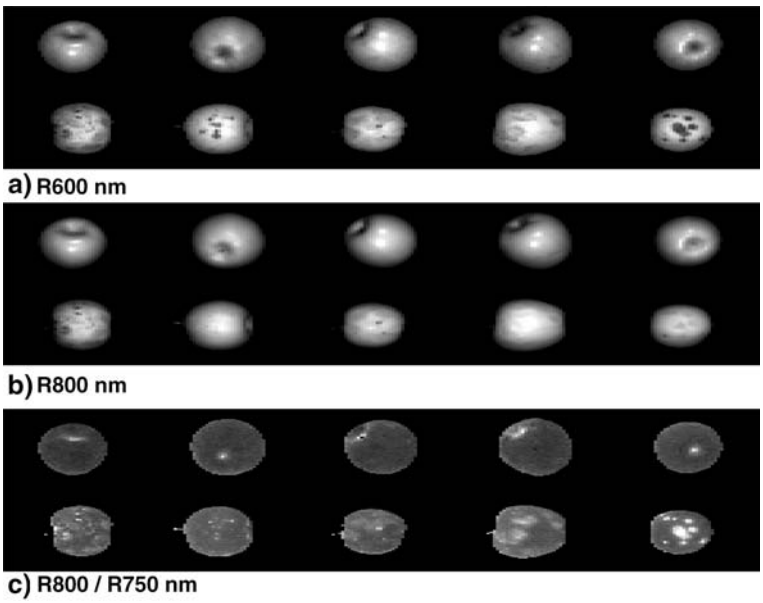

Fig. 6 Representative reflectance images; (**a**) in the visible region at 600 nm; and (**b**) in the NIR region at 800 nm. (**c**) Two NIR reflectance ratio image (800/750 nm)

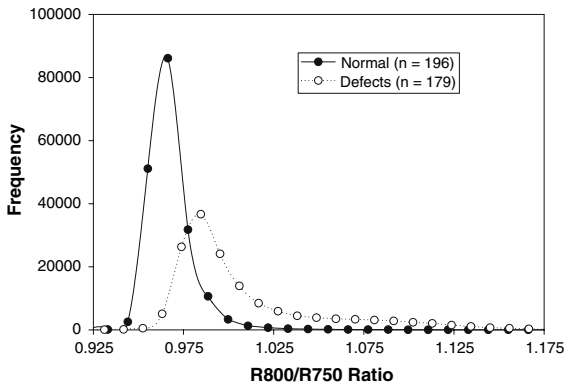

Fig. 7 Pixel intensity histogram for 800/750 nm NIR ratio for normal and defect apples

online inspection system that is capable of both of fluorescence and reflectance measurements. Furthermore, a significant implication is that it can potentially provide for current sorting mechanisms, such as by size and color, in addition to sorting for additional quality and safety attributes of products (Fig. 8). This line-scan based online imaging system is a value-added, dynamic inspection system that we believe presents a highly useful capacity for multi-tasking to meet a variety of inspection objectives. Further discussion of its potential economical benefits follows in the subsequent section.

Most importantly, it is technically feasible to simultaneously acquire multispectral combinations of both fluorescence and reflectance bands used in this investigation. The wavelengths for fluorescence (530 and 660 nm) and reflectance (750 and 800 nm) do not overlap. Thus, only UV and NIR lighting regimes for fluorescence excitation and NIR reflectance, respectively, are needed; no illumination in the visible spectrum is required. The system can be readily configured to acquire only a few selected spectral channels (in multispectral or random track mode), providing additional potential to meet other sorting requirements such as shape and other quality attributes. We have been evaluating the online system to simultaneously acquire the above multispectral reflectance and fluorescence images.

Because using the system in a multispectral configuration for a few selected channels reduces the data volume so drastically, compared to the data volume of contiguous hyperspectral bands, the data transfer time per line scan is also markedly reduced. We are also in the process of upgrading the EMCCD to a pixel readout rate greater that 30 MHz. These modifications will allow us to inspect apples moving at even higher speeds, and/or significantly improve the spatial image resolution.

Economic considerations and potential benefits

Food processing industries are well aware of food safety concerns and typically employ safe food production practices. Yet, despite the association of animal fecal matter with recent outbreaks of food-borne illness, it may not be an economically viable option for apple processors to inspect each individual apple for fecal contamination. Implementing a system dedicated to this single specific task is costly for current product processing operations. Public perception can also play an important role in that the apple processing industry (or any other food industries) may not be willing or forthcoming to proactively inspect for fecal contamination. Natural occurrences of fecal

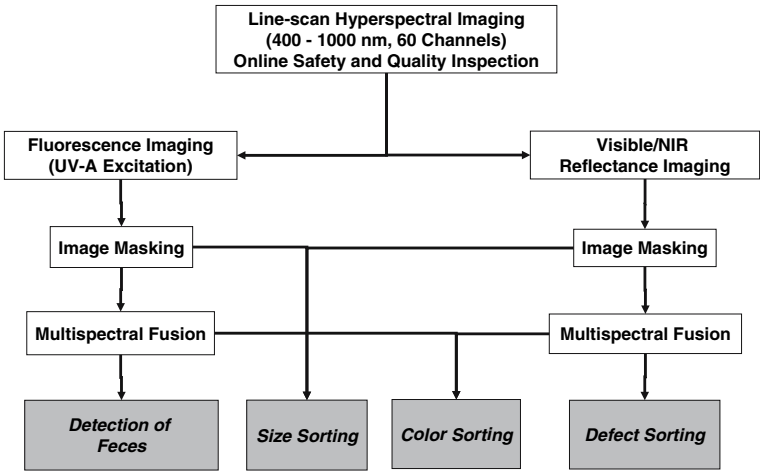

Fig. 8 A flowchart showing the potential application of both reflectance and fluorescence method for quality and safety inspection/sorting of apples

contamination on apples are very rare. But however infrequent, industry-wide significant economical losses can be expected once the problems arise, as evidenced by the recent *E. coli* contamination of spinach. Processors with a multi-tasking inspection system may gain a competitive edge in public relations for having implemented a proactive measure to further ensure safe food production.

Without government regulations, fecal contamination inspection by the apple industry would be a voluntary measure. To date, in spite of potentially huge economic losses, no industries have sought online inspection based on machine vision to potentially reduce the health and economic risks associated with fecal contamination. Processing plants currently equipped with machine vision systems only address size and color sorting. However, it is our view that a single inspection system with multi-tasking capabilities for both current sorting purposes and sorting for defects and fecal contamination cannot be ignored by industry.

Our tests of the hyperspectral line-scan imaging system with a commercial apple sorting machine have demonstrated that it can readily be integrated into current commercial systems without significant changes. The multi-tasking inspection approach described above may potentially and gradually attract industries to implement detection of fecal contamination as a voluntary measure to further reduce potential health risks and economic losses. The potential benefits may outweigh industry reluctance to adopting such science-based, multi-tasking inspection system over the current inspection regimes.

Conclusions

A hyperspectral line-scan imaging system integrated with a commercial apple-sorting machine was evaluated to detect apples for fecal contamination and defects at a processing line speed of over three apples per second. Results showed that fluorescence imaging (using a two-band ratio) could achieve detection of fecal spots on artificially contaminated apples with a 100% detection rate and no false positives regardless of the presence of defects. A NIR two-band reflectance ratio coupled with a simple classification method based on the heterogeneity of the ratio values achieved a 99.5% apple defect classification accuracy with a false positive rate of only 2%. The presented NIR processing regime overcame the presence of stem/calyx that typically has been a problematic source for false-positives in the detection of defects [13, 15, 25].

The most significant and important outcome of this investigation is the technical demonstration of a single online inspection system that is capable of both of fluorescence and reflectance measurements. It is also technically feasible to simultaneously acquire multispectral combinations of both the fluorescence and reflectance bands used in this investigation. Thus, the line-scan inspection system can potentially provide the capability for current sorting mechanisms, such as by size and color, in addition to additional sorting for quality and safety attributes of food products. This line-scan based online imaging system may offer great potential as a value-added dynamic inspection system due to its capability for multi-tasking to meet a variety of inspection objectives. A multi-tasking inspection system that can meet current industry sorting needs with the added benefit of safety inspection without requiring significant modification of existing infrastructure or incurring significant costs may lead the apple industry to consider adopting voluntary measures to further enhance safe production and processing of fruits.

With the current imaging configuration (e.g., hyperspectral), one of the factors restricting the current acquisition speed to about three apples per second is the data transfer rate (i.e., 10 MHz pixel readout rate). The system can be configured to acquire only a few select spectral channels (multispectral mode) that will markedly increase

the data transfer rate per line scan. We are also in the process of updating the EMCCD with a pixel readout rate greater that 30 MHz. These modifications may allow us to inspect apples moving at much faster speeds, over 10 apples per second.

Acknowledgements The authors would like to thank Dr. Yang Tao of University of Maryland, College Park, Maryland, for providing the apple-sorting machine. We would also like to express our gratitude to Mr. Frank Gwozdz of the FSIS, USDA, for constructing the frame for the imaging system.

References

1. P.S. Mead, L. Slutsker, V. Dietz, L.F. McCaig, J.S. Bresee, C. Shapiro, P.M. Griffin, R.V. Tauxe, Emerg. Infect. Dis. **5**, 607–625 (1999)
2. G.L. Armstrong, J. Hollingsworth, J.G. Morris, Epidemiol. Rev. **18**, 29–51 (1996)
3. S.H. Cody, M.K. Glynn, J.A. Farrar, K.L. Cairns, P.M. Griffin, J. Kobayashi, M. Fyfe, R. Hoffman, A.S. King, J.H. Lewis, B. Swaminathan, R.G. Bryant, D.J. Vugia, Ann. Intern. Med. **130**, 202–209 (1999)
4. S.L. Burnett, J. Chen, L.R. Beuchat, Appl. Environ. Microbiol. **66**, 4679–4687 (2000)
5. J. Mercier, C.L. Wilson, Biol. Control 4, 138–144 (1994)
6. K. Chao, Y.R. Chen, H. Early, B. Park, Appl. Eng. Agric. **15**(4), 363–369 (1999)
7. Z. Chen, Y. Tao, Appl. Opt. **40**(8), 1195–2000 (2001)
8. M.S. Kim, A.M. Lefcourt, Y.R. Chen, I. Kim, D.E. Chan, K. Chao, Trans. ASAE **45**(6), 2027–2037(2002a)
9. M.S. Kim, A.M. Lefcourt, Y.R. Chen, I. Kim, K. Chao, D. Chan, Trans. ASAE **45**(6), 2039–2047(2002b)
10. P.M. Mehl, Y.R. Chen, M.S. Kim, D.E. Chan, J. Food Eng. **61**(1), 67–81 (2004)
11. T.F. Schatzki, R.P. Haff, R. Young, I. Can, L.-C. Le, N. Toyofuku, Trans. ASAE **40**(5), 1407–1415 (1997)
12. M.A. Shahin, E.W. Tollner, R.W. McClendon, H.R. Arabnia, Trans. ASAE **45**(5), 1619–1627 (2002)
13. J.A. Throop, D.J. Aneshansley, W.C. Anger, D.L. Peterson, Postharvest Biol. Technol. **36**(3), 281–290 (2005)
14. C.C. Yang, K. Chao, Y.R. Chen, M.S. Kim, H.L. Early, Trans. ASABE **49**(1), 245–257 (2006)
15. B.S. Bennedsen, D.L. Peterson, Trans. ASAE. **47**(3), 889–894 (2004)
16. O. Kleynen, V. Leemans, M.-F. Destain, J. Food Eng. **69**(10), 41–49 (2005)
17. V. Leemans, M.-F. Destain, Comput. Elec. Agric. **20**(2), 117–130 (1998)
18. M.S. Kim, A.M. Lefcourt, Y.R. Chen, Appl. Opt. **42**(19), 2934–3927 (2003a)
19. M.S. Kim, A.M. Lefcourt, Y.R. Chen, T. Yang, J. Food Eng. 71(1), 85–91 (2005)
20. A.M. Lefcourt, M.S. Kim, Y.R. Chen, Appl. Optics **42**(19), 3935–3943 (2003)
21. A.M. Vargas, M.S. Kim, Y. Tao, A.M. Lefcourt, Y.R. Chen, Y. Luo, Y. Song, Y. Buchanan, J. Food Sci. **70**(8), E471–E476 (2005)
22. M.S. Kim, Y.R. Chen, P.M. Mehl, Trans. ASAE **44**(3), 721–729 (2001)
23. M.S. Kim, A.M. Lefcourt, Y.R. Chen, J. Food Prot. **66**(7), 1198–1207 (2003b)
24. P. Narayanan, A.M. Lefcourt, U. Tasch, R. Rostamian, A. Grinblat, M.S. Kim, Theoretical aspects of orienting fruit using stability properties during rotation. ASAE Meeting Presentation Portland Oregon, Paper No: 061144 (2006)
25. Z. Wen, Y. Tao, Trans. ASAE **43**(2), 446–452 (2000)